Naval Research Laboratory

Washington, DC 20375-5320

NRL/MR/5656--09-9189

Water Transmission of 1440-nm Femtosecond Pulses

David Lukofsky
Ulf Österberg

Thayer School of Engineering
Dartmouth College
Hanover, New Hampshire

Marc Currie

Photonics Technology Branch
Optical Sciences Division

April 24, 2009

Approved for public release; distribution is unlimited.

REPORT DOCUMENTATION PAGE

Form Approved
OMB No. 0704-0188

1. REPORT DATE *(DD-MM-YYYY)*
24-04-2009

2. REPORT TYPE
Memorandum Report

3. DATES COVERED *(From - To)*
23-02-2009 to 05-03-2009

4. TITLE AND SUBTITLE
Water Transmission of 1440-nm Femtosecond Pulses

5a. CONTRACT NUMBER

5b. GRANT NUMBER

5c. PROGRAM ELEMENT NUMBER

6. AUTHOR(S)
David Lukofsky,* Marc Currie, and Ulf Österberg*

5d. PROJECT NUMBER
ONR 61135N

5e. TASK NUMBER
EL011-07-43

5f. WORK UNIT NUMBER
WU 9884

7. PERFORMING ORGANIZATION NAME(S) AND ADDRESS(ES)
Naval Research Laboratory
4555 Overlook Avenue, SW
Washington, DC 20375-5320

*Thayer School of Engineering
Dartmouth College
Hanover, NH 03755

8. PERFORMING ORGANIZATION REPORT NUMBER
NRL/MR/5656--09-9189

9. SPONSORING / MONITORING AGENCY NAME(S) AND ADDRESS(ES)
Office of Naval Research
One Liberty Center
875 North Randolph Street
Arlington, VA 22203-1995

10. SPONSOR / MONITOR'S ACRONYM(S)
ONR

11. SPONSOR / MONITOR'S REPORT NUMBER(S)

12. DISTRIBUTION / AVAILABILITY STATEMENT
Approved for public release; distribution is unlimited.

13. SUPPLEMENTARY NOTES

14. ABSTRACT
This report presents the results of an experiment investigating the transmission of intense femtosecond pulses on the 1445-nm resonance of water. The goal was to detect the presence of resonant bleaching behavior, which could explain the results observed by Fox and Österberg in 2005 at the 800-nm wavelength.

15. SUBJECT TERMS
Femtosecond optical pulse
Water absorption
Optical resonance

16. SECURITY CLASSIFICATION OF: a. REPORT	b. ABSTRACT	c. THIS PAGE	17. LIMITATION OF ABSTRACT	18. NUMBER OF PAGES	19a. NAME OF RESPONSIBLE PERSON
					Marc Currie
Unclassified	Unclassified	Unclassified	UL	19	**19b. TELEPHONE NUMBER** *(include area code)* (202) 404-4201

Standard Form 298 (Rev. 8-98)
Prescribed by ANSI Std. Z39.18

Water Transmission of 1440 nm Femtosecond Pulses

1. Introduction

Our purpose was to investigate whether bleaching effects in water could sustain reduced absorption over relatively long distances. While incoherent bleaching reduces the absorption coefficient over relatively short distances, coherent bleaching - because of a continual exchange of energy between a pulse and the medium - could sustain deviations over relatively long distances. The inhomogeneous dephasing time T_2^* plays a central role in distinguishing the regime of coherent bleaching from incoherent bleaching effects. While incoherent bleaching could occur with a sufficiently intense pulse of duration $T_2', T_2^* \ll \tau \ll T_1$, coherent bleaching has the stringent requirement that $T_2^* \ll \tau \ll T_1, T_2'$.

The dephasing times of water are not precisely known, especially for the multitude of resonances present throughout the water spectrum. Nonetheless, from data available for other liquids, it is reasonable to assume that the inversion lifetime T_1 of water is much greater than 100 femtoseconds, []. Hence, the incoherent bleaching regime should be attainable with femtosecond pulses of sufficiently high peak power *if it is assumed that water behaves as a two-level system near its strongest resonances*.

The following presents the results of an experiment investigating the transmission of intense femtosecond pulses on the 1445 nm resonance of water. The goal was to detect the presence of resonant bleaching behavior, which could explain the results observed by Fox and Osterberg in 2005 at the 800 nm wavelength, [].

2. Water Approximated as a Two-Level System

The absorption coefficient of a two-level system affected by homogeneous and inhomogeneous broadening has been derived by Allen and Eberly, []. In MKS units, the absorption profile of such a medium is given by:

$$\alpha(t, z; w) = \frac{-N\omega_o\gamma^2}{4\varepsilon_o\hbar c} \int g_H(\Delta')g_I(\Delta')w(t, z; \Delta')d\Delta' \tag{1}$$

where N is the molecular density [m^{-3}], ω the resonance frequency [rad-s^{-1}], γ the dipole moment [C-m], ε_o the permittivity of free space [F-m^{-1}], $\hbar$ Planck's constant [J-s], and c the speed of light [m-s^{-1}].

In the case of a single Lorentz medium, the homogeneously broadened and inhomoge-

Manuscript approved March 27, 2009.

neously broadened lines g_H and g_I are given by:

$$g_H = \frac{1}{\pi T_2'} \frac{1}{(\omega - \omega_o)^2 + (1/T_2')^2} \tag{2}$$

$$g_I = \frac{1}{\pi T_2^*} \frac{1}{(\omega - \omega_o)^2 + (1/T_2^*)^2} \tag{3}$$

Hence, it is possible to describe a resonance in its entirety by having knowledge of the T_2' and T_2^* times, provided that neighboring resonances are far enough spectrally so to not cause additional broadening because of resonance interaction. This is an especially important point for water, Fig.(1), whose absorption profile is an aggregate of a multitude of interacting resonances. Because of this complex structure, the simple approximation of Eq.(1) could only

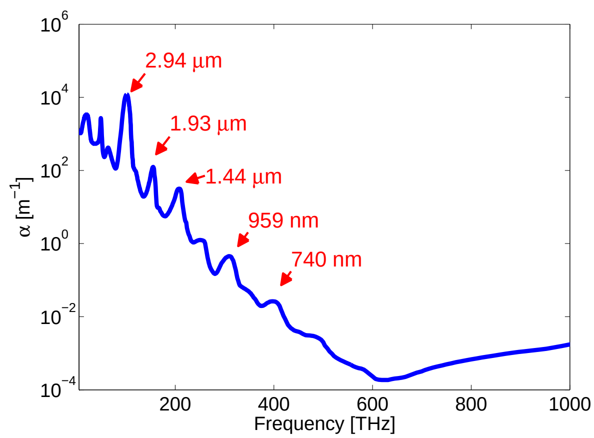

Fig. 1. Absorption coefficient of water based as measured by Segelstein, [].

model water's strongest resonances where multi-resonance interactions could be neglected.

The strongest resonance in water corresponds to the OH stretch band at 2.94μm. Stenger *et. al* report that this resonance has a homogeneous lifetime T_2' of 90 fs, and Thomas (by doing an experimental fit) reports a T_2^* of 46 fs, []. The transitional dipole moment has been determined experimentally by Callegeri *et. al* to be $\gamma = 6.2 \times 10^{-30}$C-m. Since the water density is 3.35×10^{28} molecules/m^3, it is possible to use Eq.(1) and compute a resonant absorption coefficient of $\alpha = 11681$ cm^{-1}. This computed result differs by 8% from the absorption coefficient of water measured by Segelstein, Fig.(2).

Documentation on the 1447 nm overtone resonance of water is more difficult to encounter in the literature. However, assuming that the dipole moment and homogeneous lifetimes at this wavelength are identical to the ones at 2.94μm, we obtain an inhomogeneous lifetime $T_2^* = 23$ fs by fitting absorption data, Fig.(3). These lifetimes and value for the transitional

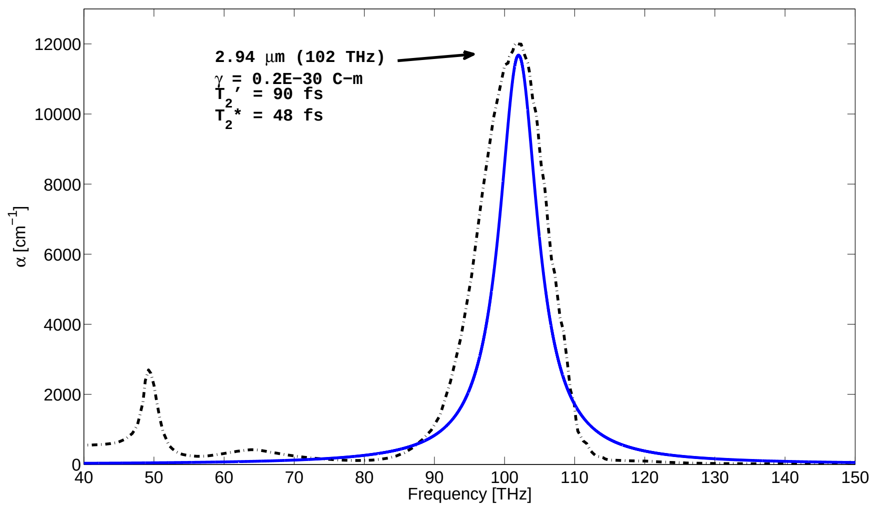

Fig. 2. Fit of the absorption peak at 1442 nm according to data from Stenger *et. al*, Thomas, and Callegeri *et. al*, [].

dipole moment make it possible to calculate the approximate threshold for coherent and incoherent bleaching. Recall that the bleaching thresholds are given by

$$I_{\text{coh. thresh.}} = \frac{\theta^2 \times 9.3 \times 10^{-72}[\mathrm{C}^2\mathrm{J\ s}]}{\gamma^2 \times \mathrm{FWHM}_I^2} \tag{4}$$

$$I_{\text{incoh. thresh.}} = \frac{2.96 \times 10^{-71}}{T_1 T_2^* \gamma^2} \tag{5}$$

Hence, the peak intensity required for incoherent bleaching is $\approx$ 77 MW/cm^2 and the peak intensity for coherent bleaching is $\approx$ 23 GW/cm^2 assuming $T_1 = 1$ ns, $T_2^* = 1$ fs and a $\mathrm{FWHM}_I = 100$ fs.

3. Experiments

The experimental setup was designed to measure transmission of optical pulses through fixed distances of water as the input pulse energy was varied. This differed from some previous absorption measurements in water that focused on the propagation of a fixed pulse energy through varying distances of water in order to investigate the $1/z$ signature decay of Brillouin precursors.

The setup consisted of a fixed sample of water, a detector measuring the beam power before the sample, a detector measuring the beam power after the sample, crossed-polarizers, filters, or a combination of both to vary the intensity of the laser pulses entering the sample,

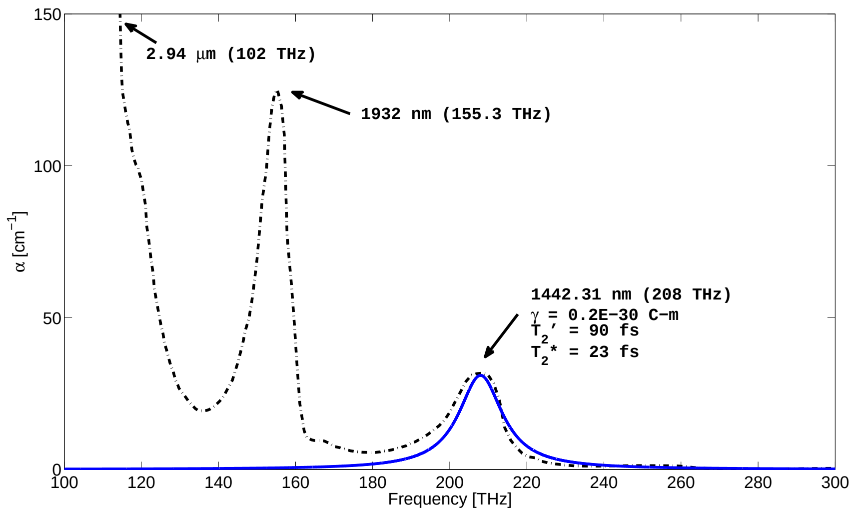

Fig. 3. Fit of the absorption peak at 1442 nm according to data from Stenger *et. al*, Thomas, and Callegeri *et. al*, [].

Fig.(4). Two detectors were used to minimize the amount of moving parts during the different iterations of the experiment, but also to insure that the transmission measurements were independent of power fluctuations in the laser cavity.

The laser system was a SpectraPhysics Hurricane Titanium:Sapphire system combined with an Spectra Physics OPA. The Hurricane systems output $\approx$ 100 fs amplified pulses at 800 nm, and the OPA was then used to tune the wavelength to the 1440 nm with a BBO crystal seeded with white light obtained by Self-Phase Modulation. The output consisted in a 1.75 mm diameter laser beam of $\approx$ 100 fs pulses of $\approx 0.1\mu$J energy at a repetition rate of 1 KHz. A sample FROG trace of the laser output going through one filter is shown in Fig.(5). The spatial profile of the beam was characterized with a knife edge, Fig.(6).

3.A. Experiment 1: Crossed-Polarizers (beam not focused)

The first experiment used crossed polarizers to attenuate the laser beam. Polarizers were chosen over filters in light of the importance of changing the laser power from iteration to iteration without changing the frequency content of the laser beam. While errors in filter calibration are eliminated by using two detectors (this type of systematic error does not affect relative power measurements), a filter subject to high enough intensities could generate new frequencies and skew the measurements. This is an especially important point for transmission measurements in frequency regions of rapidly varying absorption coefficient (such as in the vicinity of a water resonance).

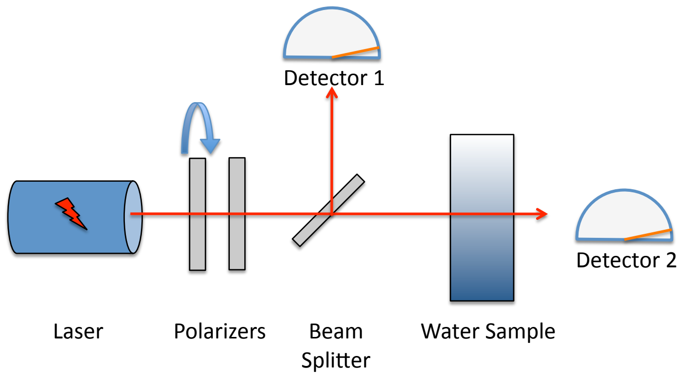

Fig. 4. A diagram of the experimental setup with two crossed-polarizers.

For this reason, and also because filters may chirp the laser pulses differently, two crossed polarizers were used as the first method to attenuate laser power, Fig.(4). This method obviously assumes that all photons in the beam have identical polarization, which is reasonable since the overwhelming majority of photons in a laser cavity are created by stimulated emission.

Fig.(7) shows the results of a transmission experiment completed with a 1.75mm in diameter laser beam with laser pulses $\approx$ 150 fs FWHM. No strong intensity dependance was noted from the results, although it was clear that the approximate transmission values for each water sample does not follow monochromatic Beer's law. Indeed, the Segelstein absorption coefficient at 1440nm is ≈ 3.2 cm^{-1}, which implies a transmission of 4.08% for the 1 mm sample, 0.17% for the 2 mm sample, 1.1×10^{-5} for the 5 mm sample and 1.266×10^{-12} for the 10 mm sample.

However, two of the four plotted results are consistent with a broadband Beer's law, where the theoretical transmission is calculated by accounting for the full bandwidth of the input spectrum. Specifically, Fig.(8) shows the input spectrum with the absorption coefficient of water as measured by Segelstein. Performing a broadband Beer's law simulation indicates that the transmitted values should be 6.2% for the 1 mm sample, 0.73% for the 2 mm sample, 0.2040% for the 5 mm sample and 0.09% for the 10 mm sample. The discrepancy between calculated and theoretical transmission for the 5 and 10 mm sample is attributed to the noise level in the measured off-resonance energy of the input spectrum. This off resonance energy is subject to much less attenuation.

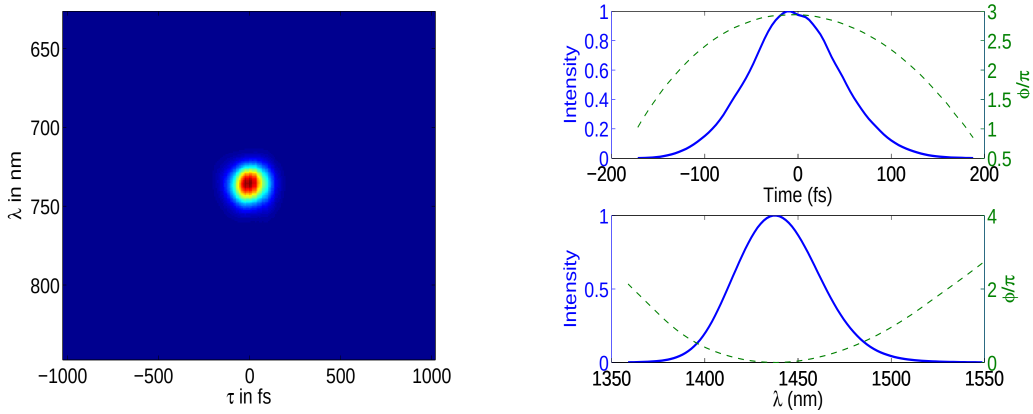

(a) FROG trace.

(b) Reconstructed pulse.

Fig. 5. A typical FROG trace from the amplified laser system and OPA.

3.B. Experiment 2: Crossed-Polarizers (focused)

The experiment was then repeated by focusing the laser beam to a diameter of approximately 18.33 μm and placing the water samples at the focal point.

A LabVIEW vi was written to collect the data automatically with a DAQ card which allowed to gather many more data points. Note that only measurements with the 2 mm and 5 mm water samples were completed. It was difficult to place the 1 mm sample at the focal point, and the power measurements of the data collected for 10 mm sample were excessively contaminated by noise. The results of the transmission experiments using the focused beam are shown in Fig.(9).

These results raised questions about the assumption that the polarizers do not affect the spectral content of the laser beam. While it appears that increasing the input energy in the 2-mm sample increased the amount of transmission, the opposite trend was noted with the 5 mm sample. This suggests that the cross-polarizer angle affected the spectral content of the beam in a non-consistent manner.

3.C. Experiment 3: Polarizers and Filters (focused beam)

This experiment used three OD filters combination (no filter, 9.5%, 0.9025%) to attenuate the incident laser beam in three large increments, and the polarizers were then crossed very slightly to gather additional data points. The intent was that crossing the polarizers very slightly would only induce negligible changes in the spectral content of the beam, and avoid the difficulties of the previous experiments.

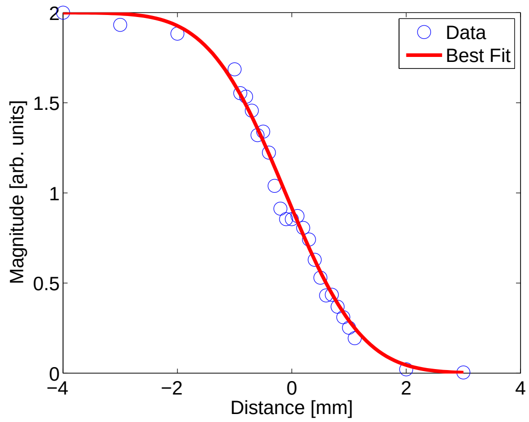

Fig. 6. Experimental and fitted knife-edge data. The FWHM is ≈ 1.75 mm.

The results of this experiment are illustrated in Fig.(11), where it is apparent that there are three clouds of points each corresponding to one of the three filters used in the experiment. This suggests that, as the polarizers are crossed to achieve the low power data point for each filter, the spectral content of the beam is modified such that off-resonance frequencies were blocked more than on-resonance frequencies. Nonetheless, despite this effect of the polarizers, the data suggests that there is a trend of increase in transmission as the power of the beam entering the sample is increased.

3.D. Experiment 4: Filters Only (focused beam)

In light of the inconsistencies encountered with the crossed-polarizers, the experiment was repeated with filters only. This limited the number of data points to approximately seven. Again, to take advantage of the full dynamic range of the detectors, filters were also used in front of the detector area. The results of the unfocused experiment are shown in Fig.(12). The results of the focused experiment are shown in Fig.(13).

Different filter combinations were characterized with the FROG method to determine their effect on pulse shape. This is particularly important since different layers of filters had to be used to achieve the desired intensity levels of the experiment. However, the FROG measurements demonstrated that the filters caused only negligible chirp on the pulses, which is consistent with the low-dispersion of glass in the 1440 nm region. A typical FROG trace is shown in Fig.(5).

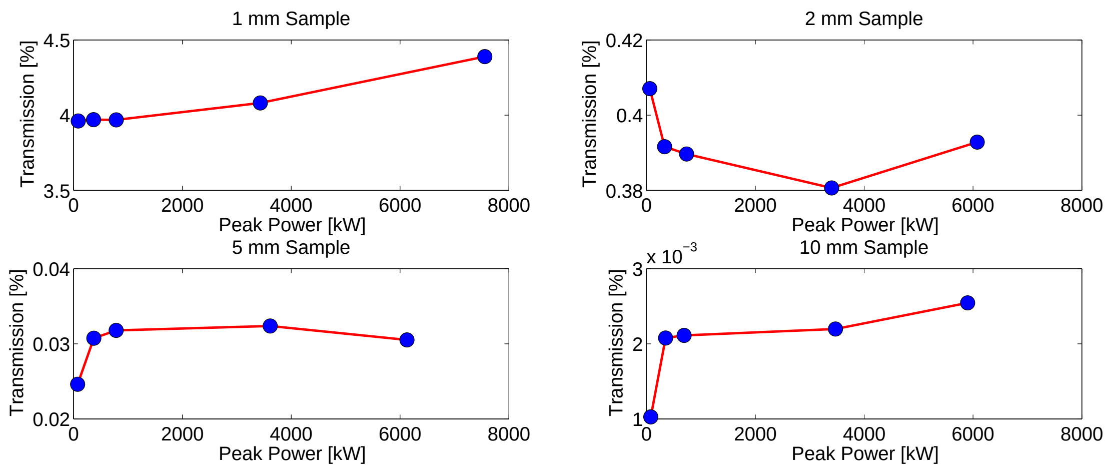

Fig. 7. Results of the 1440 nm transmission experiments for different water distances as a function of input peak power. The beam diameter for these experiments was 1.75 mm.

Filter Combination	**Temporal Width**	**Spectral Width**	**FROG Error**
OD 3.0	112 fs	53 nm	0.31%
OD 3.0 & OD 0.1	- fs	- nm	-%
OD 3.0 & OD 0.3	110 fs	53 nm	0.38%
OD 3.0 & OD 3.0	117 fs	50 nm	0.23%

3.E. Experiment 5: Filters Only (focused beam and no water)

The focused experiment was repeated but with no water in the samples, Fig.(14).

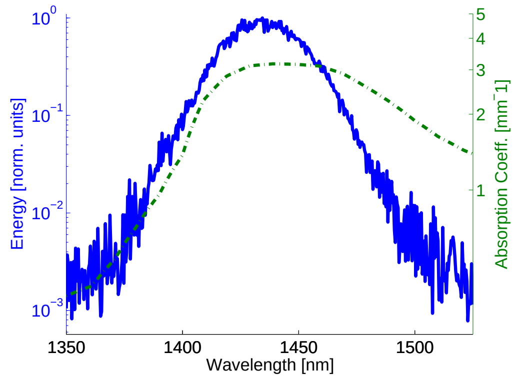

Fig. 8. The spectrum of the beam at the input of the experiment with the Segelstein absorption coefficients.

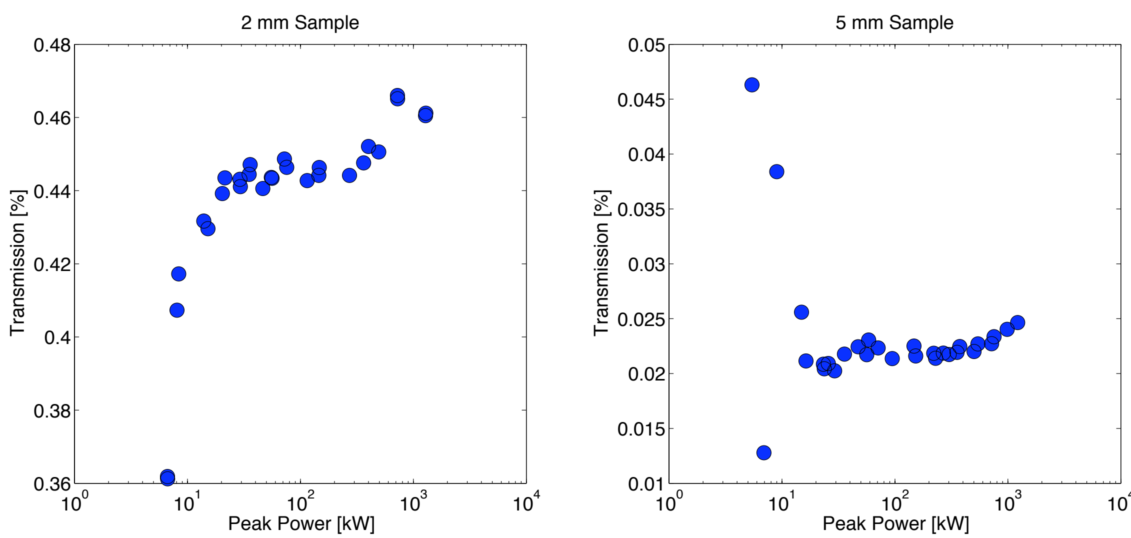

Fig. 9. Results of the 1440 nm transmission experiments for different water distances as a function of input peak power. The beam diameter for these experiments was $18.33\mu m$.

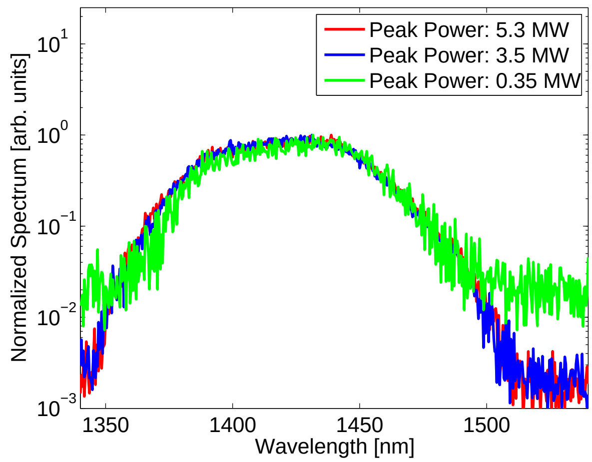

Fig. 10. Change of the spectrum as the polarizers are crossed.

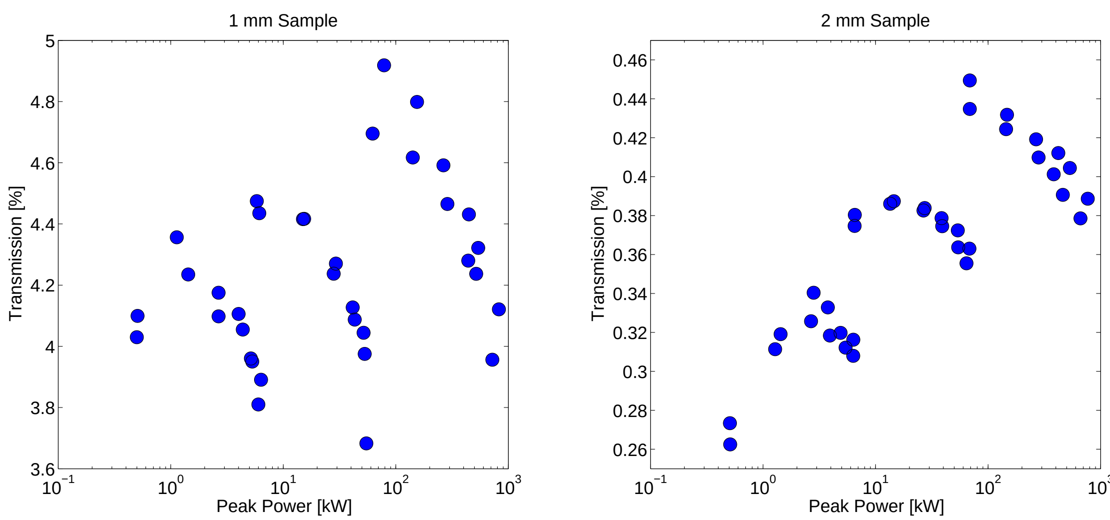

Fig. 11. Results of the 1440 nm transmission experiments for different water distances as a function of input peak power. The beam diameter for these experiments was 18.33μ mm.

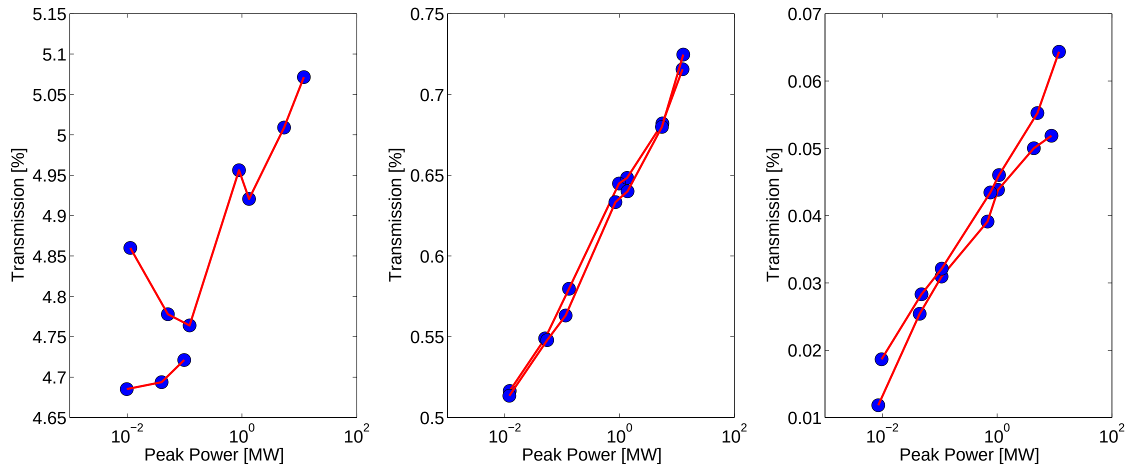

Fig. 12. Results of the 1440 nm transmission experiments for different water distances as a function of input peak power by using filters only. The beam radius at the focus was 1.75 mm.

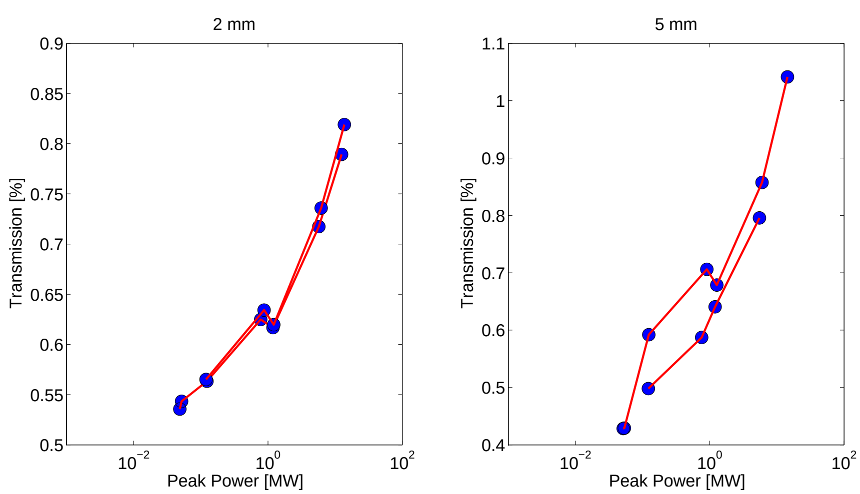

Fig. 13. Results of the focused 1440 nm transmission experiments for different water distances as a function of input peak power. The beam radius at the focus was $18.33\mu m$.

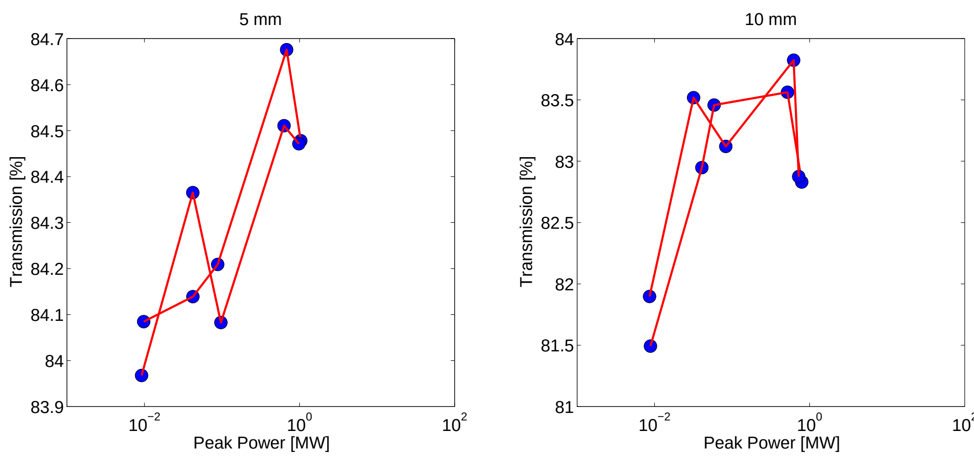

Fig. 14. Transmission measurements through glass samples with no water.

Experimental Setup 1

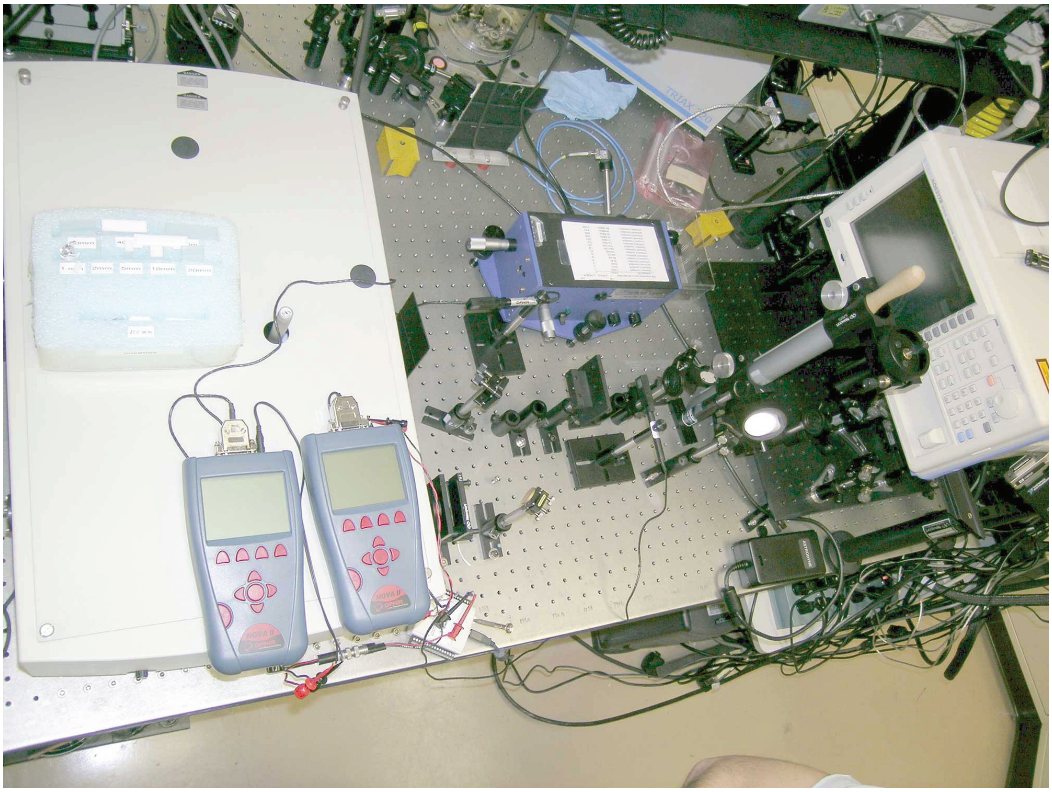

Experimental Setup 2

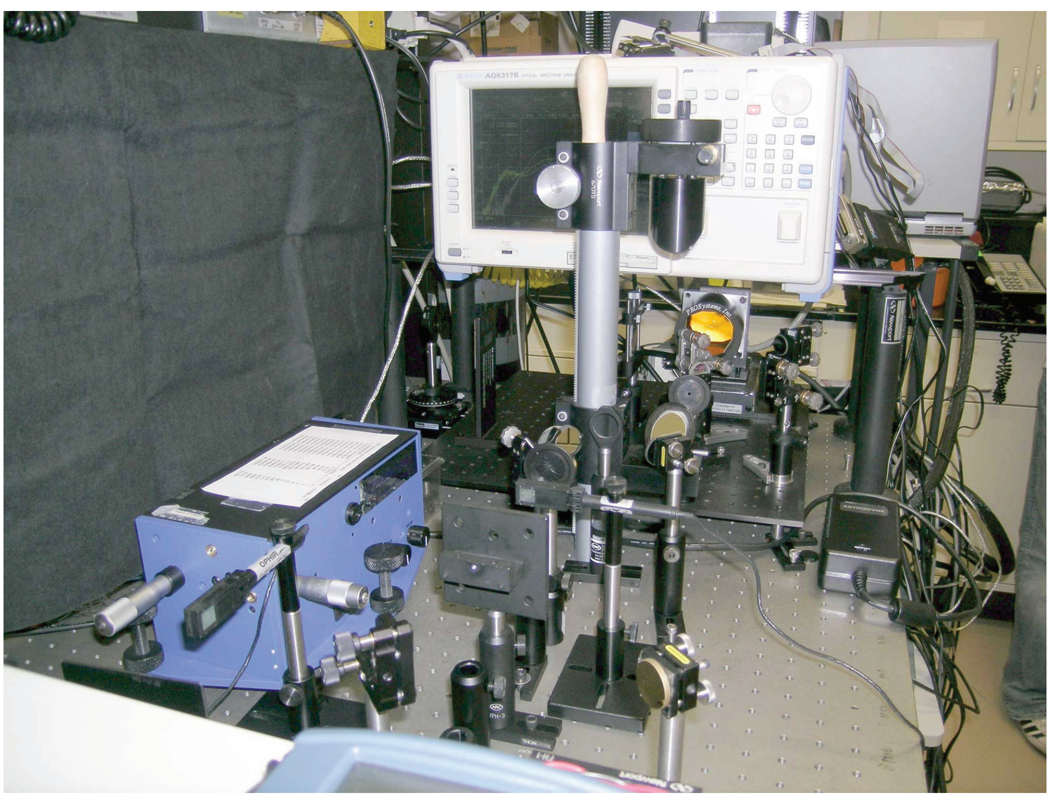

Experimental Setup 3

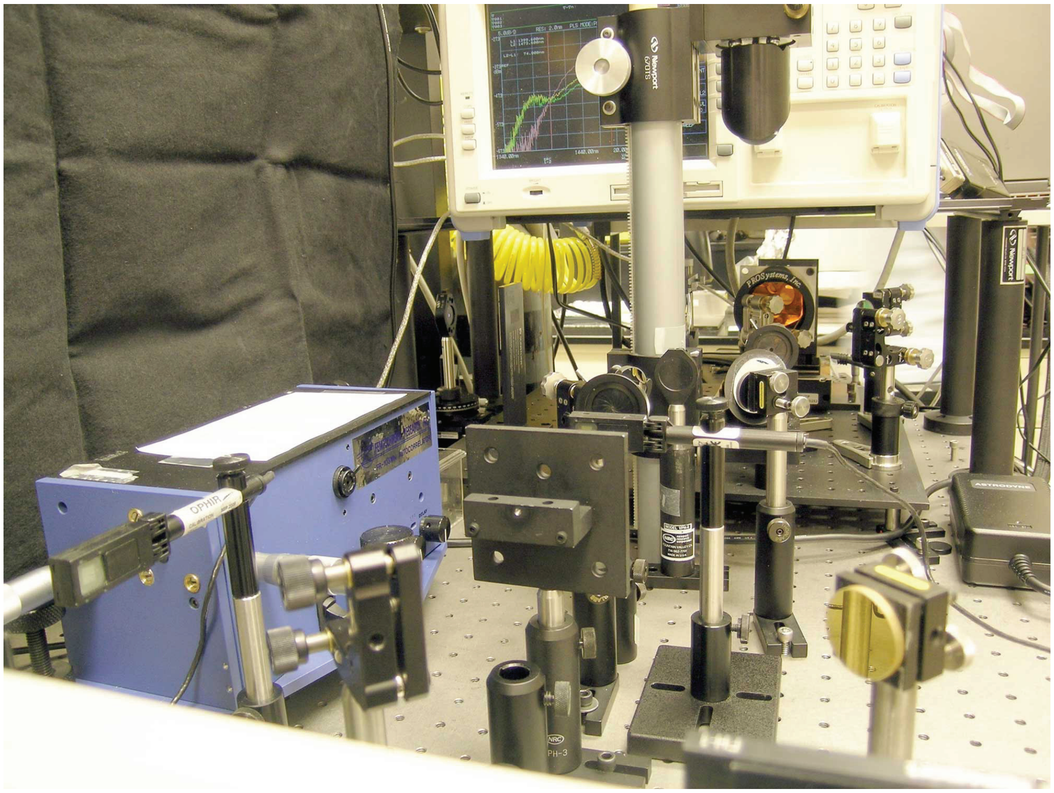

Experimental Setup 4

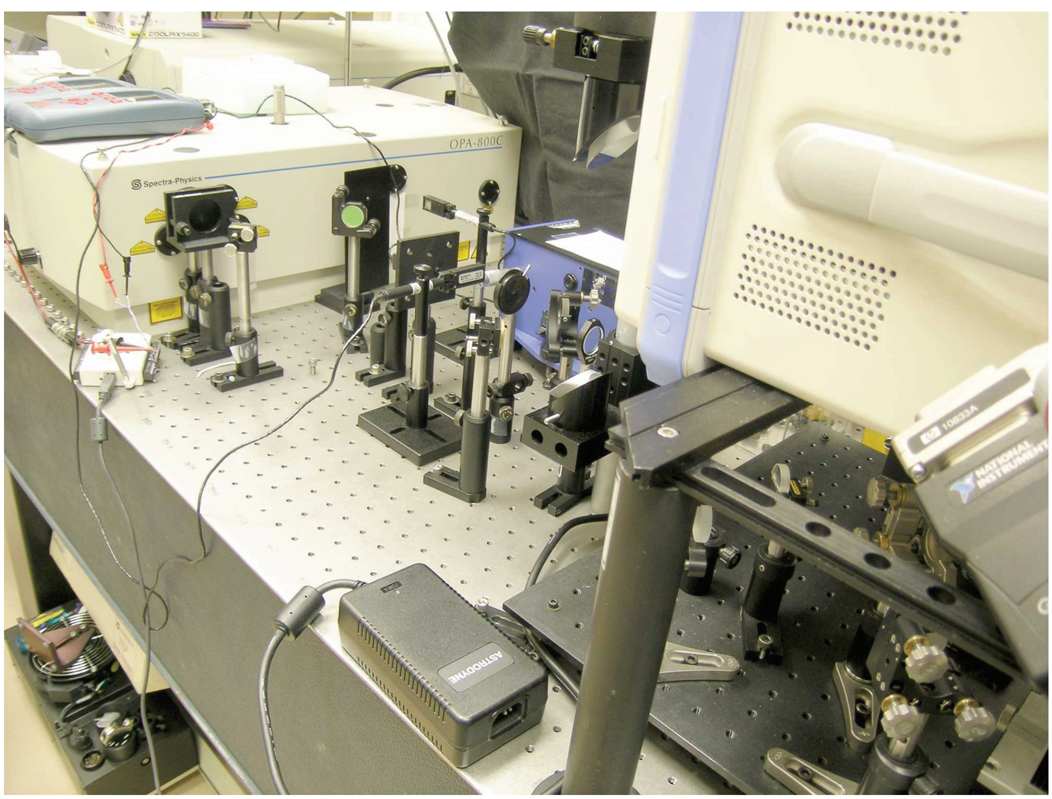

Experimental Setup 5

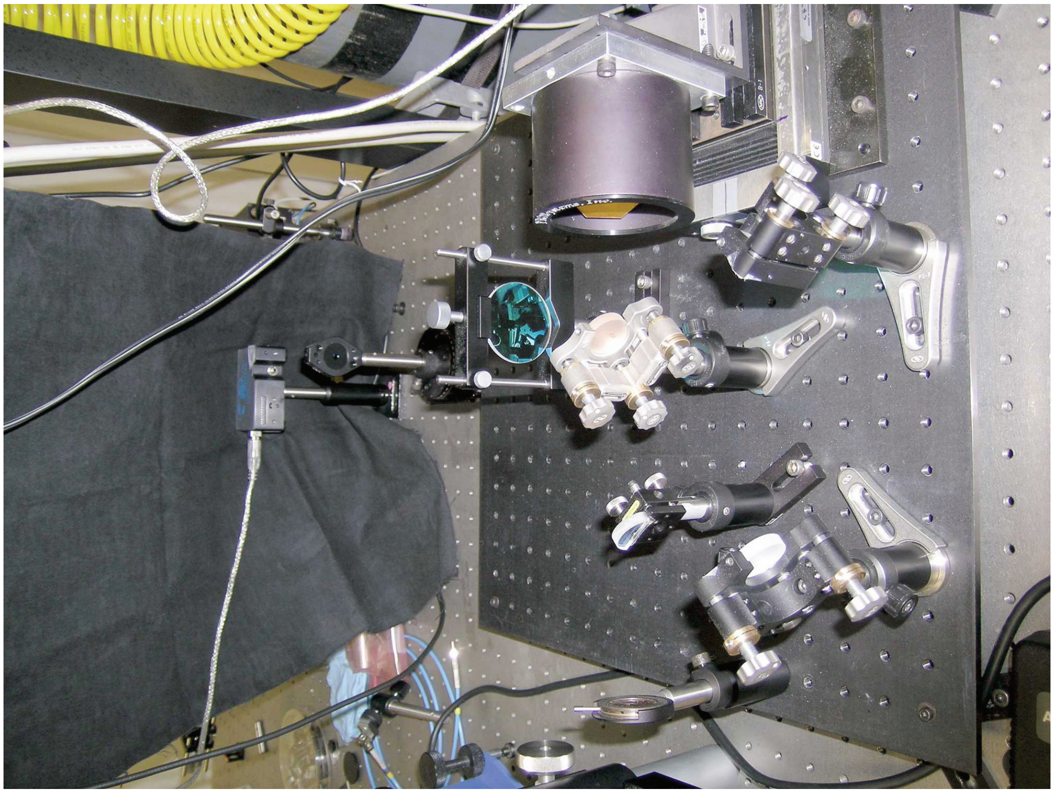

Experimental Setup 6

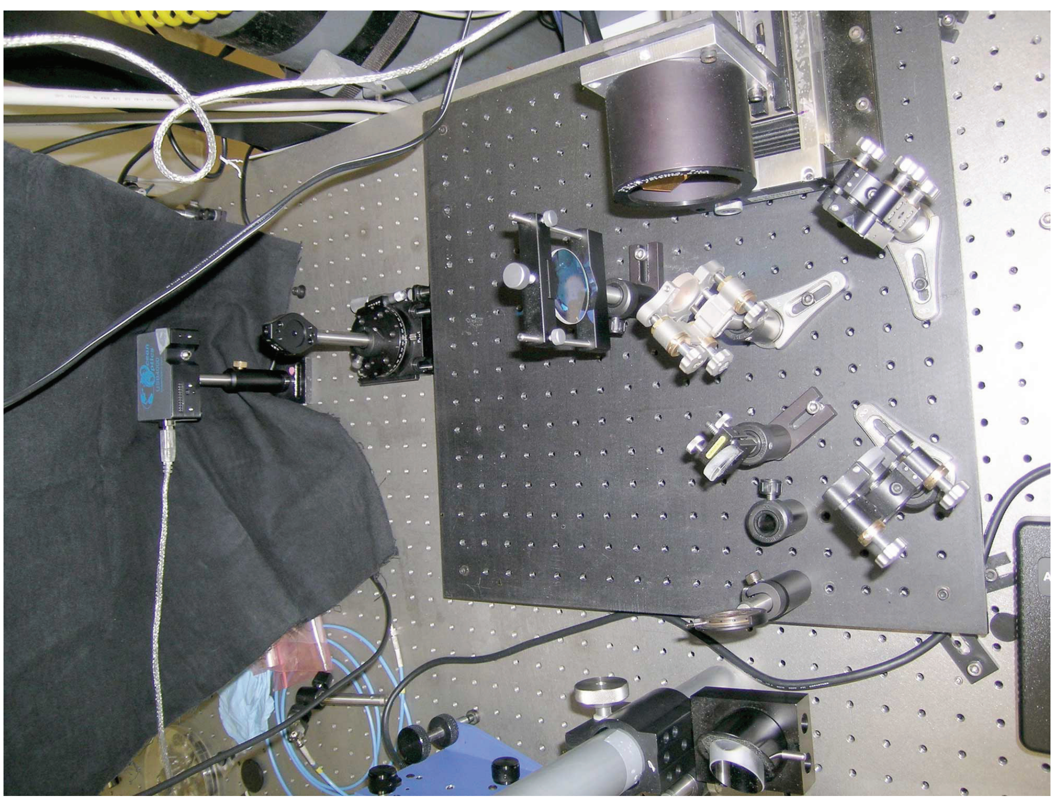

Experimental Setup 7

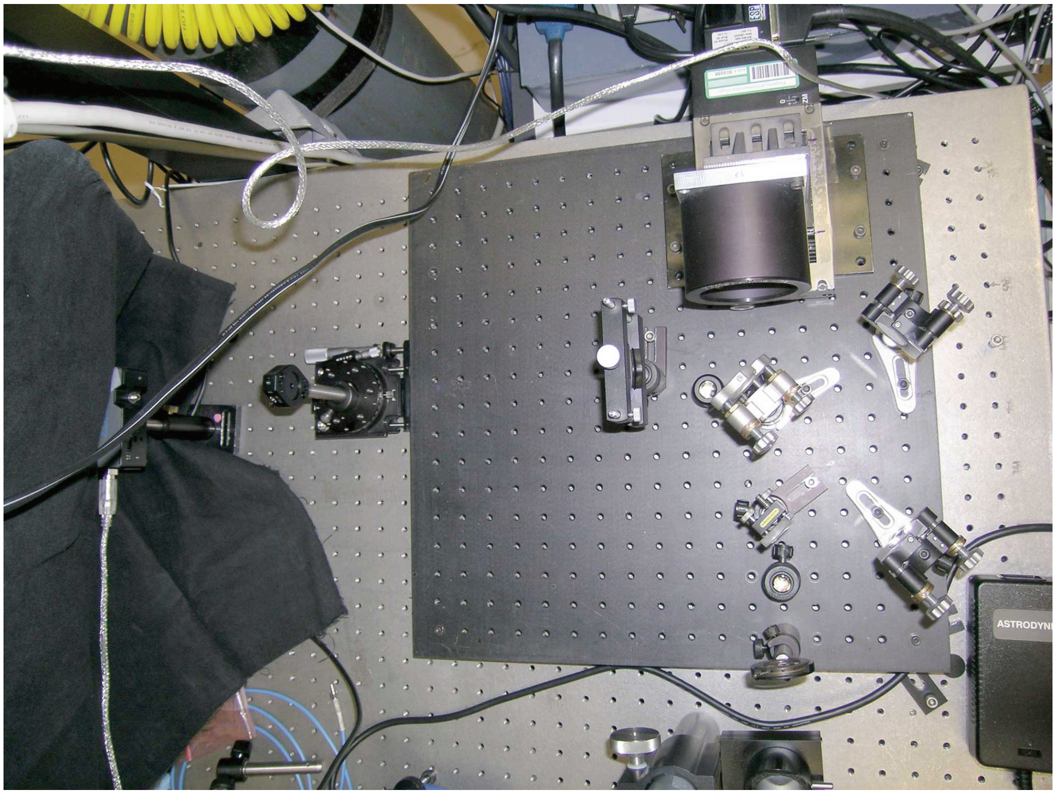

Experimental Setup 8

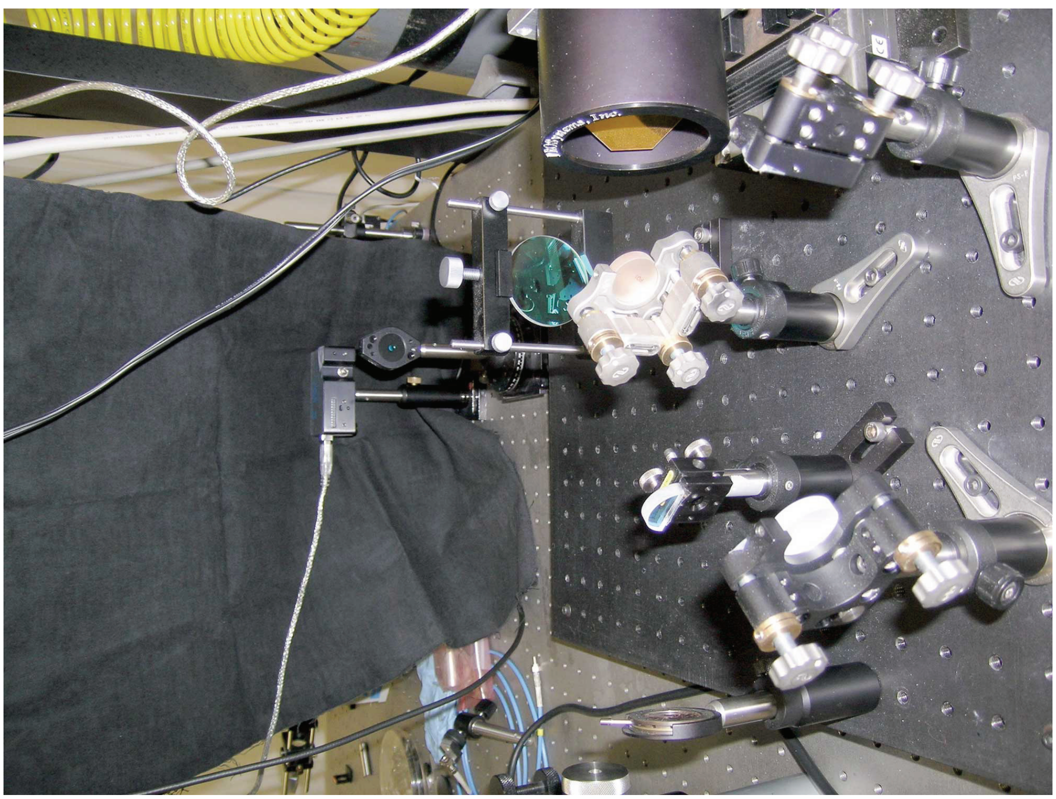

Experimental Setup 9